Article

The pH Dependent Nuclearity Variation of {Mo}-type Polyoxomolybdates and Tectonic Effect on Their Aggregations

Sayaka Shishido, and Tomoji Ozeki

J. Am. Chem. Soc., **2008**, 130 (32), 10588-10595 • DOI: 10.1021/ja800784a • Publication Date (Web): 22 July 2008

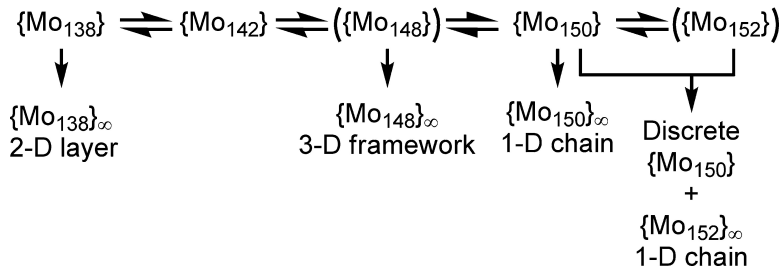

More About This Article

Additional resources and features associated with this article are available within the HTML version:

- Supporting Information
- Access to high resolution figures
- Links to articles and content related to this article
- Copyright permission to reproduce figures and/or text from this article

View the Full Text HTML

J|A|C|S
ARTICLES

Published on Web 07/22/2008

The pH Dependent Nuclearity Variation of $\{Mo_{154-x}\}$-type Polyoxomolybdates and Tectonic Effect on Their Aggregations

Sayaka Shishido and Tomoji Ozeki*

Department of Chemistry and Materials Science, Tokyo Institute of Technology, 2-12-1-H-63 O-okayama, Meguro-ku, Tokyo 152-8551, Japan

Received January 31, 2008; E-mail: tozeki@cms.titech.ac.jp

Abstract: The pH dependence of the structures of $\{Mo_{154-x}\}$ mixed-valence oxomolybdate giant clusters were investigated by synchrotron X-ray diffraction of systematically prepared crystals containing $[Mo_{138}O_{410}(OH)_{20}(OH_2)_{46}]^{40-}$ (**1**), $[Mo_{138}O_{410}(OH)_{20}(OH_2)_{38}]^{40-}$ (**2**), $[Mo_{138}O_{406}(OH)_{16}(OH_2)_{46}]^{28-}$ (**3**), $[Mo_{142}O_{400}(OH)_{52}(OH_2)_{38}]^{28-}$ (**4**), $[Mo_{142}O_{432}(OH_2)_{58}]^{40-}$ (**5**), $[Mo_{148}O_{436}(OH)_{15}(OH_2)_{56}]^{27-}$ (**6**), $[Mo_{150}O_{451}(OH)_5(OH_2)_{61}]^{35-}$ (**7**), and both $[Mo_{150}O_{442.5}(OH)_{11.5}(OH_2)_{64}]^{24.5-}$ and $[Mo_{152}O_{446}(OH)_{20}(OH_2)_{54}]^{28-}$ (**8**). Crystals **1**, **4**, and **5** contain discrete clusters while intercluster Mo−O−Mo bonds connect the clusters into chains in crystal **7**, into two-dimensional networks in crystals **2** and **3**, and into a three-dimensional framework structure in crystal **6**. Crystal **8** contains both discrete and linearly catenated clusters: discrete $\{Mo_{150}\}$ are located between the chains of $\{Mo_{152}\}$. Direct correlation was observed between the nuclearity of the clusters with the pH of the mother liquor. On the other hand, the geometries of extended structures do not show apparent correlation with the pH. They turned out to be governed by the tectonics of the component clusters. The pH of the mother liquor exerts influence on the extended structure through the structures of the constituent clusters.

Introduction

Current increasing research activities in polyoxometalate chemistry[1–3] have led to the development of novel compounds with potential or realized functionalities, for example, as catalysts,[4] magnetic materials,[5] and small molecule storing materials.[6] Synthetic strategies for such compounds largely depend on the knowledge of the chemical behaviors of polyoxometalates.[7] The past decade saw an explosion of the research on a new class of polyoxometalates, the high-nuclearity mixed-valence molybdenum giant clusters with the sizes measuring typically several nanometers.[8–11] They are promising candidates as precursors or building blocks for the syntheses of even larger structures and hybrid materials with different kinds of compounds. Since rational designs of such substances require the knowledge of the chemical behaviors of the component giant cluster polyoxometalates, its further accumulation deserves significant importance.

Typical examples of giant cluster polyoxomolybdates with distinct structural types are spherical $\{Mo_{132}\}$,[12,13] ring-shaped $\{Mo_{154}\}$[14] and $\{Mo_{176}\}$,[15,16] and lemon-shaped $\{Mo_{368}\}$,[17,18] of which the $\{Mo_{154}\}$ family has the largest number of derivatives.[19–33]

(1) Pope, M. T., Müller, A., Eds. *Polyoxometalate Chemistry: From Topology via Self-Assembly to Applications*; Kluwer Academic Publishers: Dordrecht, The Netherlands, 2001.
(2) Yamase, T., Pope, M. T., Eds. *Polyoxometalate Chemistry for Nano-composite Design*; Kluwer Academic/Plenum Publishers: New York, 2002.
(3) Borrás-Almenar, J. J., Coronado, E., Müller, A., Pope, M., Eds. *Polyoxometalate Molecular Science*; Kluwer Academic Publishers: Dordrecht, The Netherlands, 2003.
(4) Botar, B.; Geletii, Y. V.; Kögerler, P.; Musaev, D. G.; Morokuma, K.; Weinstock, I. A.; Hill, C. L. *J. Am. Chem. Soc.* **2006**, *128*, 11268–11277.
(5) Nellutla, S.; van Tol, J.; Dalal, N. S.; Bi, L.-H.; Kortz, U.; Keita, B.; Nadjo, L.; Khitrov, G. A.; Marshall, A. G. *Inorg. Chem.* **2005**, *44*, 9795–9806.
(6) Jiang, C.; Lesbani, A.; Kawamoto, R.; Uchida, S.; Mizuno, N. *J. Am. Chem. Soc.* **2006**, *128*, 14240–14241.
(7) See, for example: Pope, M. T. *Heteropoly and Isopoly Oxometalates*; Springer: Berlin, 1983.
(8) Müller, A.; Kögerler, P. *Coord. Chem. Rev.* **1999**, *182*, 3–17.
(9) Müller, A.; Serain, C. *Acc. Chem. Res.* **2000**, *33*, 2–10.
(10) Müller, A.; Kögerler, P.; Dress, A. W. M. *Coord. Chem. Rev.* **2001**, *222*, 193–218.
(11) Müller, A.; Roy, S. *Coord. Chem. Rev.* **2003**, *245*, 153–166.
(12) These high nuclearity clusters are often referred to as $\{Mo_x\}$ without specifying the identity and the number of the ligands, especially when their nuclearities are of central interest. A certain moiety of the cluster is similarly named, for example, $\{Mo_2\}$ for a portion of the cluster with two Mo centers. This convention is adopted in this paper.
(13) Müller, A.; Krickemeyer, E.; Bögge, H.; Schmidtmann, M.; Peters, F. *Angew. Chem., Int. Ed.* **1998**, *37*, 3360–3363.
(14) Müller, A.; Krickemeyer, E.; Meyer, J.; Bögge, H.; Peters, F.; Plass, W.; Diemann, E.; Dillinger, S.; Nonnenbruch, F.; Randerath, M.; Menke, C. *Angew. Chem., Int. Ed. Engl.* **1995**, *34*, 2122–2124.
(15) Müller, A.; Krickemeyer, E.; Bögge, H.; Schmidtmann, M.; Beugholt, C.; Kögerler, P.; Lu, C. *Angew. Chem., Int. Ed.* **1998**, *37*, 1220–1223.
(16) Jiang, C.-C.; Wei, Y.-G.; Liu, Q.; Zhang, S.-W.; Shao, M.-C.; Tang, Y.-Q. *Chem. Commun.* **1998**, 1937–1938.
(17) Müller, A.; Beckmann, E.; Bögge, H.; Schmidtmann, M.; Dress, A. *Angew. Chem., Int. Ed.* **2002**, *41*, 1162–1167.
(18) Müller, A.; Botar, B.; Das, S. K.; Bögge, H.; Schmidtmann, M.; Merca, A. *Polyhedron* **2004**, *23*, 2381–2385.
(19) Müller, A.; Das, S. K.; Fedin, V. P.; Krickemeyer, E.; Beugholt, C.; Bögge, H.; Schmidtmann, M.; Hauptfleisch, B. *Z. Anorg. Allg. Chem.* **1999**, *625*, 1187–1192.
(20) Müller, A.; Das, S. K.; Bögge, H.; Beugholt, C.; Schmidtmann, M. *Chem. Commun.* **1999**, 1035–1036.
(21) Müller, A.; Das, S. K.; Kuhlmann, C.; Bögge, H.; Schmidtmann, M.; Diemann, E.; Krickemeyer, E.; Hormes, J.; Modrow, H.; Schindler, M. *Chem. Commun.* **2001**, 655–656.
(22) Müller, A.; Roy, S.; Schmidtmann, M.; Bögge, H. *Chem. Commun.* **2002**, 2000–2002.

10.1021/ja800784a CCC: $40.75

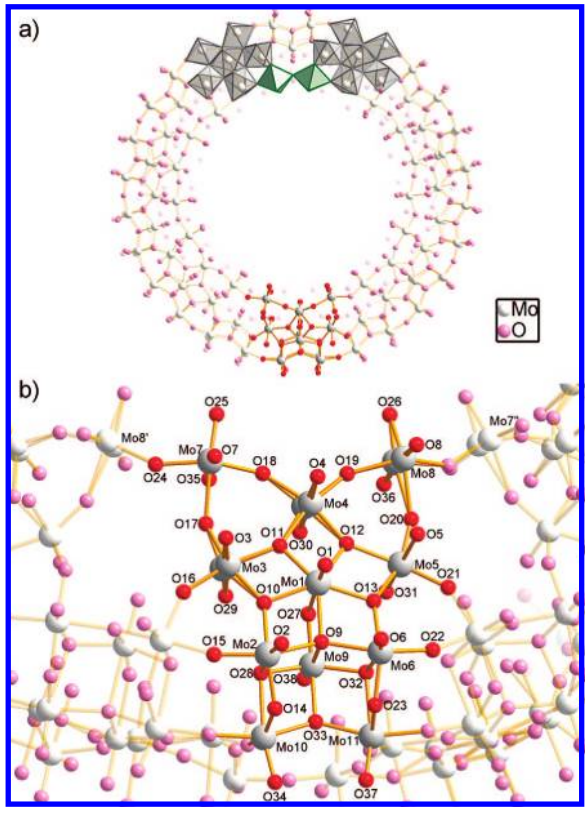

Figure 1. (a) Structure of $\{Mo_{154}\}$ viewed along its axle. A $\{Mo_{11}\}$ repeating unit at the bottom is highlighted by showing Mo and O atoms with gray and red spheres. Two $\{(Mo)Mo_5\}$ pentagonal units and a $\{Mo_2\}$ linker between them are also highlighted by showing their MoO_x coordination spheres in gray and green polyhedra. (b) A $\{Mo_{11}\}$ repeating unit with the numbering scheme of its Mo and O atoms. All the atoms of $\{Mo_{154-x}\}$ in crystals **1**−**8** are commonly labeled with a numeric code designating the position of the atom in the repeating unit followed by an alphabetical ID designating the position of the repeating unit in the whole cluster (A−D in crystal **1**−**5** and **7**, A−G in crystal **6**, and A−G and H−N in crystal **8**, as shown in Figures 2–7). In the $\{Mo_{11}\}$ unit shown here, Mo3, Mo4, and Mo8 are disordered over two sites. Mo8′ and Mo7″ belong to neighboring repeating units.

The $\{Mo_{154}\}$ cluster approximates to D_{7d} symmetry with 14 $\{Mo_{11}\}$ repeating units of C_s symmetry, as shown in Figure 1. It has several characteristic moieties that define the structural features of its derivatives, among which are fourteen $\{(Mo)Mo_5\}$ pentagonal units (Mo1−Mo6), fourteen $\{Mo_2\}$ linkers (Mo7 + Mo8′ and Mo8 + Mo7″, Mo8′ and Mo7″ belong to neighboring repeating units) that link two $\{(Mo)Mo_5\}$ units, and fourteen $\{Mo_1\}$ moieties (Mo9) that are located inside of the ring. Defects of $\{Mo_2\}$ and $\{Mo_1\}$ moieties are responsible for the formation of fewer nuclearity derivatives. A survey of hitherto reported structurally characterized $\{Mo_{154}\}$ derivatives with their key synthetic parameters and the resultant structural features is summarized in Table S1. While roughly one-third of them have all their 154 Mo sites fully occupied,[14,19–23] others have defect molybdenum sites and thus have a fewer number of molybdenum atoms: to the best of our knowledge, crystal structures of $\{Mo_{152}\}$,[19,24] $\{Mo_{150}\}$,[25] $\{Mo_{146}\}$,[19] $\{Mo_{144}\}$,[24,26] $\{Mo_{142}\}$,[27–31] $\{Mo_{140}\}$,[32] and $\{Mo_{138}\}$[33] species have been reported. These series of clusters remind us of the lacunary derivatives of the Keggin[34] and Dawson[35] polyoxometalates, where the proton concentration of the synthetic condition determines the nuclearity. Similarly, the nuclear growth of a $\{Mo_{154-x}\}$ family member by the gain of a $\{Mo_2\}$ linker unit can be interpreted as a proton-consuming dehydration reaction and could be formulated as follows:

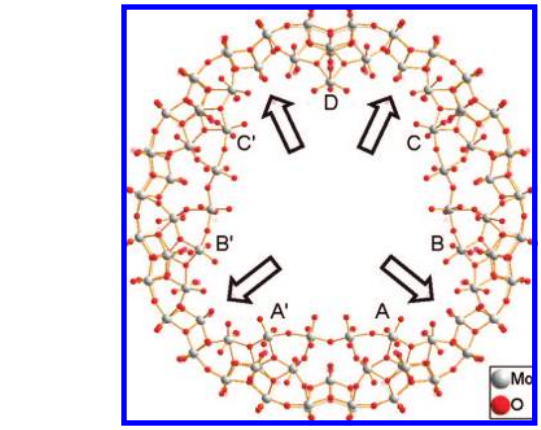

Figure 2. Structure of $\{Mo_{138}\}$ in crystal **1**. The back side of the ring is shown dimmed for clarity. Arrows indicate the defect $\{Mo_2\}$ sites. The $\{(Mo)Mo_5\}$ in the repeating unit D misses two $\{Mo_2\}$ linkers on its both sides. Units A′−C′ are related to units A−C by the crystallographic mirror plane.

$$[H_pMo_{154-x}O_{532-y}]^{q-} + 2MoO_4^{2-} + 2H^+ \underset{OH^-}{\overset{H^+}{\rightleftharpoons}} [H_pMo_{154-x+2}O_{532-y+7}]^{(q+2)-} + H_2O \quad (1)$$

In fact, higher nuclearity compounds tend to be synthesized in strongly acidic conditions, and lower nuclearity ones in weakly acidic conditions. However, there are several exceptions; for example, whereas a $\{Mo_{154}\}$ ring was prepared at pH 1.5,[21] a $\{Mo_{144}\}$ ring was prepared at pH 0.8.[26] Other factors that have been reported to affect the nuclearity include reaction time,[27,29] reaction temperature,[28] concentration of Mo,[19,24] electron donor and its redox potential,[24,29] and/or other substances present in the system.[24,28] Effects of these factors seem to have obscured the pH dependence of the nuclearity of the $\{Mo_{154-x}\}$ rings.

Another intriguing feature of the $\{Mo_{154}\}$ family polyoxometalates is the ability to condense into higher-order structures, that is, one-dimensional chain[19,22–24,26] and two-dimensional network[20,24] structures. Formation of such extended structures

(23) Yamase, T.; Prokop, P.; Arai, Y. *J. Mol. Struct.* **2003**, *656*, 107–117.
(24) Müller, A.; Krickemeyer, E.; Bögge, H.; Schmidtmann, M.; Beugholt, C.; Das, S. K.; Peters, F. *Chem.—Eur. J.* **1999**, *5*, 1496–1502.
(25) Yamase, T.; Ishikawa, E.; Abe, Y.; Yano, Y. *J. Alloys Compd.* **2006**, *408*−*412*, 693–700.
(26) Müller, A.; Krickemeyer, E.; Bögge, H.; Schmidtmann, M.; Peters, F.; Menke, C.; Meyer, J. *Angew. Chem., Int. Ed. Engl.* **1997**, *36*, 484–486.
(27) Müller, A.; Beugholt, C.; Koop, M.; Das, S. K.; Schmidtmann, M.; Bögge, H. *Z. Anorg. Allg. Chem.* **1999**, *625*, 1960–1962.
(28) Müller, A.; Krickemeyer, E.; Bögge, H.; Schmidtmann, M.; Kögerler, P.; Rosu, C.; Beckmann, E. *Angew. Chem., Int. Ed.* **2001**, *40*, 4034–4037.
(29) Yamase, T.; Prokop, P. V. *Angew. Chem., Int. Ed.* **2002**, *41*, 466–469.
(30) Yamase, T.; Yano, Y.; Ishikawa, E. *Langmuir* **2005**, *21*, 7823–7832.
(31) Botar, B.; Kögerler, P.; Hill, C. L. *J. Am. Chem. Soc.* **2006**, *128*, 5336–5337.
(32) Yang, W.; Lu, C.; Lin, X.; Wang, S.; Zhuang, H. *Inorg. Chem. Commun.* **2001**, *4*, 245–247.
(33) Müller, A.; Maiti, R.; Schmidtmann, M.; Bögge, H.; Das, S. K.; Zhang, W. *Chem. Commun.* **2001**, 2126–2127.
(34) Tézé, A.; Hervé, G. *J. Inorg. Nucl. Chem.* **1977**, *39*, 999–1002.
(35) Contant, R.; Ciabrini, J.-P. *J. Chem. Res. (S)* **1977**, 222; *J. Chem. Res. (M)* **1977**, 2601−2617.

Table 1. Crystal Data for **1**−**8**

	1	2	3	4	5	6	7	8
temperature (K)	35	123	123	35	123	123	123	123
crystal system	monoclinic	monoclinic	monoclinic	monoclinic	monoclinic	monoclinic	monoclinic	triclinic
space group	*C*2/*m*	*C*2/*m*	*C*2/*m*	*C*2/*m*	*C*2/*m*	*C*2/*c*	*C*2/*m*	P$\bar{1}$
crystal size (μm^3)	20 × 20 × 10	40 × 30 × 20	40 × 40 × 10	60 × 60 × 10	100 × 100 × 20	80 × 80 × 10	200 × 200 × 20	200 × 100 × 20
Z	2	2	2	2	2	4	2	1
a (Å)	30.3344(4)	26.9098(6)	27.7619(5)	42.148(4)	42.0599(7)	59.1887(5)	33.4487(5)	30.1630(5)
b (Å)	49.5012(7)	42.9546(14)	42.6994(10)	40.138(5)	40.0450(5)	47.1521(5)	53.5509(10)	34.0804(4)
c (Å)	29.0565(4)	29.4850(9)	30.2459(7)	26.191(3)	22.5450(3)	31.8640(3)	26.6741(5)	46.7339(7)
α (deg)	90	90	90	90	90	90	90	93.9918(7)
β (deg)	96.785(1)	94.283(1)	95.858(1)	69.620(4)	94.587(1)	70.305(1)	72.8254(10)	94.4527(9)
γ (deg)	90	90	90	90	90	90	90	95.3700(10)
V (Å^3)	43325(1)	33987(2)	35667(1)	41535(8)	37851(1)	83726(1)	45648(1)	47542(1)
R_{int}	0.0878	0.1069	0.0871	0.0979	0.0609	0.0863	0.0720	0.0712
$R1[Fo^2>2\sigma(Fo^2)]$	0.0672	0.0695	0.0630	0.1201	0.0564	0.0838	0.0743	0.1209

Table 2. Preparative Conditions and Key Structural Features of Crystals **1**−**8**

	pH of mother liquor	nuclearity[a]	estimated formula of the cluster	connectivity of the clusters	number of intercluster bonds per cluster[b]
1	4.5∼3.0	138/476	$[Mo_{138}O_{410}(OH)_{20}(OH_2)_{46}]^{40-}$	discrete	0
2	3.3	138/468	$[Mo_{138}O_{410}(OH)_{20}(OH_2)_{38}]^{40-}$	2-D network	4 × 4
3	3.0	138/468	$[Mo_{138}O_{406}(OH)_{16}(OH_2)_{46}]^{28-}$	2-D network	4 × 4
4	3.3∼2.5	142/490	$[Mo_{142}O_{400}(OH)_{52}(OH_2)_{38}]^{28-}$	discrete	0
5	2.2	142/490	$[Mo_{142}O_{432}(OH_2)_{58}]^{40-}$	discrete	0
6	1.7	148/507	$[Mo_{148}O_{436}(OH)_{15}(OH_2)_{56}]^{27-}$	3-D framework	6 × 2
7	1.4	150/517	$[Mo_{150}O_{451}(OH)_5(OH_2)_{61}]^{35-}$	1-D chain	2 × 2
8	1.4	150/518 and 152/520	$[Mo_{150}O_{442.5}(OH)_{11.5}(OH_2)_{64}]^{24.5-}$ and $[Mo_{152}O_{446}(OH)_{20}(OH_2)_{54}]^{28-}$	discrete {Mo_{150}} and 1-D chain {Mo_{152}}	0 and 2 × 5

[a] Represented as (number of Mo atoms)/(number of O atoms). [b] Represented as (number of connections for each cluster) × (number of bonds at each connection).

can also be interpreted as a proton-consuming dehydration reaction and formulated as follows (*r* stands for the number of Mo−O−Mo bonds connecting two {Mo_{154-x}} rings):

$$2[H_pMo_{154-x}O_{532-y}]^{q-} + 2rH^+ \underset{OH^-}{\overset{H^+}{\rightleftharpoons}} [\{H_pMo_{154-x}O_{532-y-r}\}_2O_r]^{(2q-2r)-} + rH_2O \quad (2)$$

Besides the effect of proton, the condensation reaction of the clusters have been discussed in conjunction with various factors: depletion of highly negative charge of the clusters by the substitution of terminal Mo−NO groups with Mo=O groups,[26] presence of La^{3+} cations,[23] and the destruction the hydration shell of the cluster by the use of urea.[22]

This situation highlights the importance of investigating the pure dependence on pH of the defect formation and the condensation of the {Mo_{154-x}} rings in a system as simple as possible by excluding redundant influencing components. In this context, we carried out a series of crystal structure analyses of the samples crystallized from systematically prepared solutions differing only in pH and containing only essential components for the ring formation: Mo source, acid, and reducing agent. As the acid, we employed hydrochloric acid since carboxylic[33] and sulfuric[36] acids are known to be captured into the giant ring polyoxometalates. Hydrazinium dichloride was used as the reducing agent since its oxidized form has never been incorporated into the giant clusters. $(NH_4)_6Mo_7O_{24}\cdot 4H_2O$ was employed as the Mo source since alkaline metal cations sometimes show significant influence to the structure.[31] Although these restrictions to the system lead to the difficulty in growing crystals large enough for single crystal diffraction experiments, exploitation of the high-flux X-rays from synchrotron radiation enabled their successful structure determinations. Here we report the pH dependence on the nuclearity and the extended structure formation of {Mo_{154-x}} family clusters based on the structures of eight crystals containing {Mo_{138}}, {Mo_{142}}, {Mo_{148}}, {Mo_{150}}, and {Mo_{152}}.

Results

Sample Preparations. From aqueous solutions dissolving ammonium paramolybdate and hydrazinium dichloride adjusted to various pH values with hydrochloric acid, eight crystals containing {Mo_{154-x}} anions with various nuclearity (x = 16, 12, 6, 4, and 2) were precipitated as ammonium salts. Their crystal data are summarized in Table 1. Under such a broad range of synthetic conditions, single crystals with sufficient size for X-ray diffraction may not always be easily obtained. Especially, crystal **1** measured only 20 μm × 20 μm × 10 μm. Systematic structure determinations of these crystals were enabled by the exploitation of synchrotron radiation. The reaction pH and key structural features are summarized in Table 2. While the nuclearity of the clusters show direct correlation with the mother liquor from which the crystals were precipitated, correlation between the pH and the connectivity of the clusters in the crystals is not obvious.

Crystal Structures. All the crystals **1** to **8** contain {Mo_{154-x}} family giant clusters. A decrease in their nuclearity due to the loss of {Mo_2} groups leads to the loss of the 7-fold symmetry of the parent {Mo_{154}} cluster. Highest possible symmetry of the fewer nuclearity derivatives is C_{2h} where only one C_2 axis and one σ_d plane are retained.

Crystal **1** contains a discrete {Mo_{138}} ring located on the 2/*m* site at the origin of the unit cell. It is the lowest nuclearity species of {Mo_{154-x}} family clusters with only one equal

(36) Müller, A.; Toma, L.; Bögge, H.; Schmidtmann, M.; Kögerler, P. *Chem. Commun.* **2003**, 2000–2001.

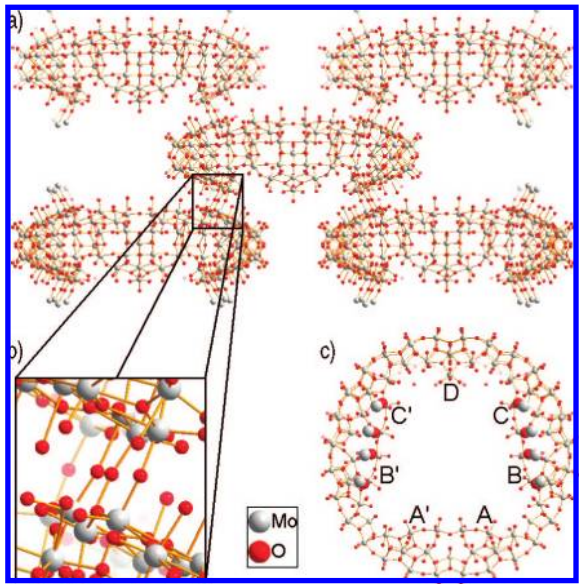

Figure 3. (a) Two-dimensional layer structure of {Mo_{138}} clusters in crystal **2**; (b) intercluster connection in crystal **2**; (c) structure of {Mo_{138}} in **2**. The oxygen atoms contributing to the intercluster connections and Mo atoms in the next cluster that bond to them are shown with larger spheres.

nuclearity member, $[Mo_{138}O_{416}H_6(H_2O)_{58}(CH_3CO_2)_6]^{32-}$, where six {$Mo_2$} and four {$Mo_1$} moieties are missing.[33] On the other hand, defects of {Mo_{138}} in **1** are observed only in {Mo_2} linker sites and thus eight {Mo_2} linkers are missing as shown in Figure 2, which is the largest number of {Mo_2} defects among hitherto structurally characterized {Mo_{154-x}} family clusters. Since the {Mo_{154}} structure has fourteen {Mo_2} linker sites at two sets of seven circularly arranged positions, occurrence of eight defect sites inevitably leads to at least two sets of two linkers located side by side. Thus the pentagonal {(Mo)Mo_5} unit between them lacks two {Mo_2} linkers on its both sides, which was proposed to be unstable.[30,33] Although a similar situation is expected for {Mo_{140}} where seven {Mo_2} linkers are missing,[32] the defect linker sites are disordered there. Therefore, the {Mo_{138}} in **1** stands as the first fully structurally characterized example with a pentagonal {(Mo)Mo_5} unit missing two {Mo_2} linkers on its both sides.

Crystal **2** contains a {Mo_{138}} ring located on the 2/*m* site at the origin of the unit cell. The {Mo_{138}} in **2** lacks eight {Mo_2} linkers, the arrangement of which is identical with that of {Mo_{138}} in **1**. The anion is connected to four symmetry related anions located at ($^1/_2$, $^1/_2$, 0), ($^1/_2$, $-^1/_2$, 0), ($-^1/_2$, $^1/_2$, 0), and ($-^1/_2$, $-^1/_2$, 0), giving rise to a two-dimensional layer structure parallel to the crystallographic *ab* plane. Each connection consists of four Mo−O−Mo bonds that involve two Mo atoms of a {Mo_2} moiety and two Mo atoms of the pentagonal {(Mo)Mo_5} units on its both sides (Mo4 and Mo8 of unit B and Mo4 and Mo7 of unit C), as shown in Figure 3. In spite of the formation of the intercluster connections, the packing of the {Mo_{138}} rings in crystal **2** is very close to that of crystal **1**, and these compounds crystallize in the same space group type *C*2/*m* with very close lattice constants for *c* and β. On the other hand, *a* and *b* of crystal **2** are significantly smaller than those of **1**, reflecting the intercluster aggregations.

Crystal **3** contains a {Mo_{138}} ring located on the 2/*m* site at the origin of the unit cell. The anion is connected to four symmetry related anions located at ($^1/_2$, $^1/_2$, 0), ($^1/_2$, $-^1/_2$, 0), ($-^1/_2$, $^1/_2$, 0), and ($-^1/_2$, $-^1/_2$, 0), giving rise to a layer structure

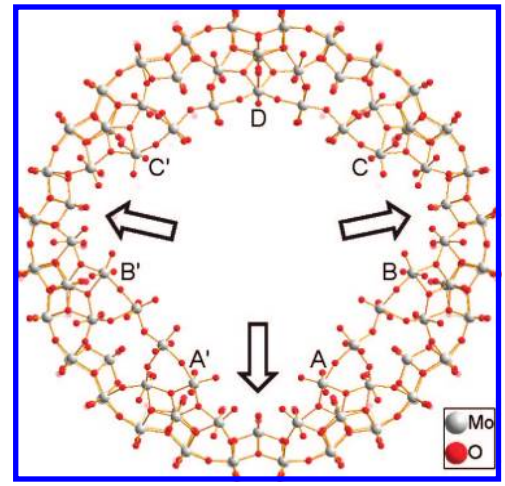

Figure 4. Structure of {Mo_{142}} in crystal **4**. The back side of the ring is shown dimmed for clarity. Arrows indicate the defect {Mo_2} sites. This structure can be obtained by filling a {Mo_2} linker to the defect between the units C and D of {Mo_{138}} shown in Figure 2, followed by a $2\pi/7$ counterclockwise rotation.

same as that in crystal **2**. While the distribution of the defect {Mo_2} linkers and the intercluster connection mode of crystal **3** are the same as those of crystal **2**, the total number of protons attached to the clusters is different between these two crystals.

Crystal **4** contains a discrete {Mo_{142}} ring that is located on the 2/*m* site at the origin of the unit cell. The {Mo_{142}} ring has eight {Mo_2} linkers and six defects, whose distribution is the same as those in the $[NH_3iPr]^+$ and Na^+ salts of {Mo_{142}}[27,29] and the NH_4^+ salt of acetate containing {$Mo_{138}(CH_3CO_2)_6$}.[33] The distribution of the {Mo_2} linkers can be obtained by simply putting a {Mo_2} linker to one of the adjoining two defect sites at each side of the {Mo_{138}} cluster, as shown in Figure 4. It may be noteworthy that the crystal packing of **4** is very close to that of {$Mo_{138}(CH_3CO_2)_6$}: both crystallize in space group *C*2/*m* with unit cell dimensions very close to each other and exhibit very similar arrangements of the clusters. It implies the crystal packing is dominated by the structures of the external moieties of the cluster, such as the distribution of the existence and absence of the {Mo_2} linkers. The difference in the internal moieties, that is, the defect of the {Mo_1} moieties and the coordination of the acetate ligands, does not seem to influence the packing very much.

Crystal **5** contains a discrete {Mo_{142}} ring with 6 {Mo_2} defects on the 2/*m* site at the origin of the unit cell. Although its metal−oxygen connectivity is the same as that of {Mo_{142}} in crystal **4**, the numbers of protons attached to these clusters are different. Crystals **4** and **5** show very similar packing patterns.

Crystal **6** contains a {Mo_{148}} ring that is located on the $\bar{1}$ site at ($^1/_4$, $^1/_4$, 0) of the unit cell. The anion is connected to six symmetry related anions centered at ($^1/_4$, $-^1/_4$, $-^1/_2$), ($^1/_4$, $-^1/_4$, $^1/_2$), ($^1/_4$, $^3/_4$, $-^1/_2$), ($^1/_4$, $^3/_4$, $^1/_2$), ($-^1/_4$, $^1/_4$, $-^1/_2$) and ($^3/_4$, $^1/_4$, $^1/_2$), to form a three-dimensional framework structure, as shown in Figure 5. During the structure refinement, six {Mo_2} linker sites that are located at three consecutive sites on each side of the ring showed lower occupancies, which were refined to approximately 0.5 and were fixed at exactly $^1/_2$ during the final stages of the refinement. Therefore, the total number of defect {Mo_2} linkers is three and the nuclearity of the cluster is 148, which has been the only missing even number nuclearity between 138 and 154 reported for structurally characterized

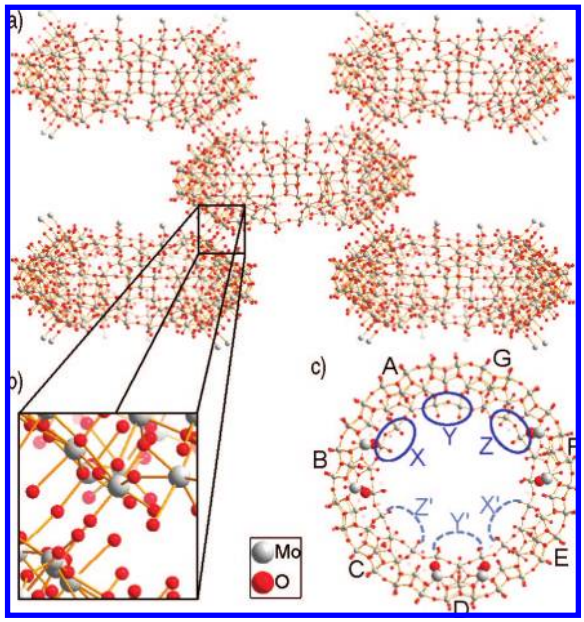

Figure 5. (a) A slice parallel to the crystallographic *bc* plane of the three-dimensional network structure of {Mo_{148}} clusters in crystal **6**. (b) Intercluster connection in crystal **6**. (c) Structure of {Mo_{148}} in **2**. The oxygen atoms contributing to the intercluster connections and Mo atoms in the next cluster that bond to them are shown with larger spheres. Site occupancies of X, Y, and Z {Mo_2} linkers are 0.5. X′, Y′, and Z′ indicate their symmetry related positions on the back side of the ring.

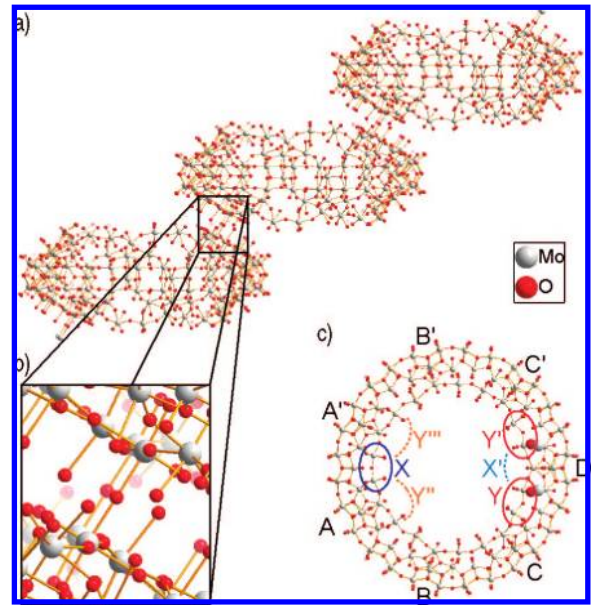

Figure 6. (a) Linear chain structure of {Mo_{150}} clusters in crystal **7**. (b) Intercluster connection in crystal **7**. (c) Structure of {Mo_{150}} in **7**. The oxygen atoms contributing to the intercluster connections and Mo atoms in the next cluster that bond to them are shown with larger spheres. Site occupancies are 0.5 for linker X and 0.75 for linker Y. Linkers X′, Y′, Y″, and Y‴ are their symmetry equivalents.

{Mo_{154-x}} family clusters (see Table S1). Selection of 3 defects out of these 6 sites gives 10 possible combinations, 8 of which are 4 sets of enantiomeric pairs. The condition that no defects come next to each other can only be satisfied with the defect combination of X + Z + Y′ (C_s symmetry), X + Z + X′ (C_1 symmetry) and its enantiomer, of which only the C_s structure can lead to the occupancy of $^1/_2$ at site Y. This arrangement of the existence and absence of the {Mo_2} linker sites cannot be obtained by a simple addition of three {Mo_2} linkers to the {Mo_{142}} structure: dissociation of at least one {Mo_2} linker is necessary during the formation of {Mo_{148}} from {Mo_{142}}. Each intercluster connection involves two Mo−O−Mo bonds from two {Mo_2} linkers on the both sides of a {(Mo)Mo_5} unit (Mo7 and Mo8 of a {Mo_{11}} repeating unit). However, the site occupancies of two out of six such {Mo_2} linkers are 0.5 and therefore the clusters are connected by only one Mo−O−Mo bond at these connections.

Crystal **7** contains a {Mo_{150}} ring that is located on the 2/*m* site at the origin of the unit cell. The anion is connected to two symmetry related anions centered at (0, 0, −1) and (0, 0, 1), to form a linear chain structure along the crystallographic *c* axis, as shown in Figure 6. During the structure refinement, six {Mo_2} linkers showed lower occupancies. Their occupancies converged to ca. 0.5 and 0.75 and were fixed exactly at $^1/_2$ and $^3/_4$ as shown in Figure 6c. Therefore, the nuclearity of the cluster is 150, corresponding to two defect {Mo_2} linker sites per cluster. Selection of two defects out of these six sites gives seven possible combinations, four of which are two sets of enantiomeric pairs. Among these, only one enantiomeric pair (e.g., an anion with defects at sites Y and Y″ in Figure 6) can be obtained by simply adding a {Mo_2} to {Mo_{148}} in crystal **6**. However, this structure cannot explain the existence of defect at site X. Defect at site X clearly proves that not only additions of but also dissociations of the {Mo_2} linkers are necessary to obtain {Mo_{150}} in crystal **7** from {Mo_{148}} in crystal **6**. Each intercluster connection involves two Mo−O−Mo bonds from two {Mo_2} linkers on the both sides of a {(Mo)Mo_5} unit (Mo7 and Mo8 of unit D). However, the site occupancies of these Mo atoms are 0.75 and therefore the clusters are connected by only one Mo−O−Mo bond at the probability of 0.5.

Crystal **8** contains {Mo_{150}} and {Mo_{152}} rings that are located on the $\bar{1}$ site at the body center and the origin of the unit cell, as shown in Figure 6. The anion centered at ($^1/_2$, $^1/_2$, $^1/_2$) is discrete and has no intercluster connections. On each side of the ring, two adjoining linkers show the occupancy of 0.75 and one of its neighboring linkers shows the occupancy of 0.5. Therefore, total number of {Mo_2} defects for the cluster becomes two, leading to the nuclearity of the cluster of 150. There are seven ways for the selection of two defect sites from the six possible sites, of which four are two sets of enantiomeric pairs. On the other hand, in the {Mo_{152}} anion at the origin, one independent {Mo_2} linker (connecting units M and L in Figure 7) shows the site occupancy of 0.5, leading to the nuclearity of the cluster of 152. It is connected to its symmetry equivalent anions centered at (1, 0, 0) and (−1, 0, 0), to form a linear chain structure along the crystallographic *a* axis. Each connection involves five Mo−O−Mo bonds originating from three Mo atoms of a {(Mo)Mo_5} unit (Mo3, Mo4 and Mo5) and Mo atoms from two {Mo_2} linkers on its both sides (Mo7 and Mo8).

Discussion

pH Dependence of the Anion Structures. Comparing the structures of **1**−**8**, the pH dependence of the nuclearity of the anions is clearly observed. When the solution pH is above 3, {Mo_{138}} is obtained. When the pH goes down to 2, {Mo_{142}} becomes predominant. When the pH is below 2, {Mo_{148}}, {Mo_{150}}, and {Mo_{152}} were obtained. The ring without defects, {Mo_{154}}, was not obtained under the conditions surveyed in this study. This trend demonstrates that the nuclearity of {Mo_{154-x}} family clusters is dominated by the acidity of the reaction

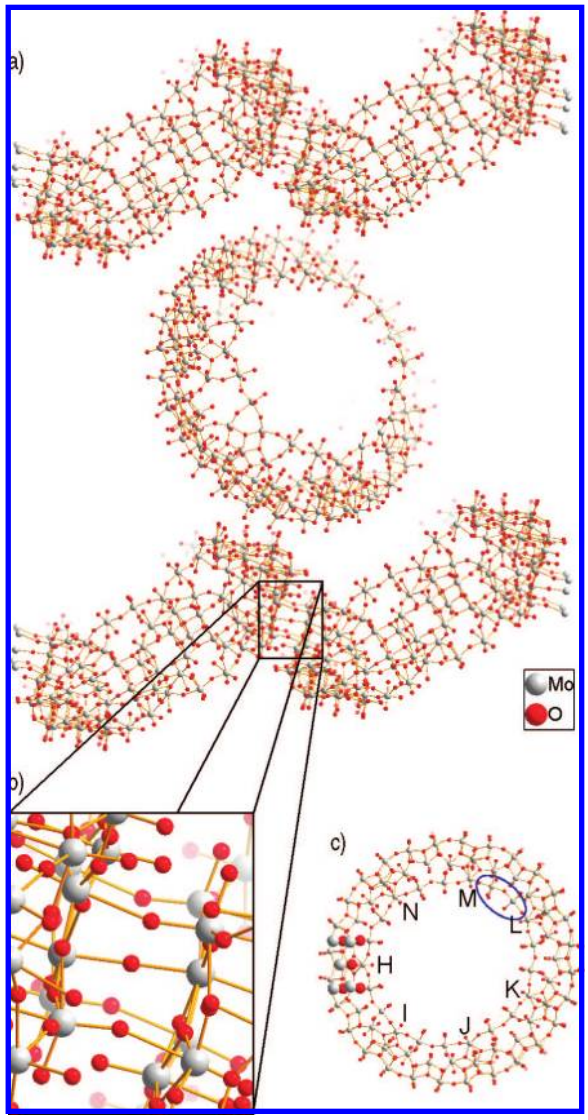

Figure 7. (a) Linearly catenated {Mo_{152}} and interstitial {Mo_{150}} clusters in crystal **8**. (b) Intercluster connection of {Mo_{152}} in crystal **8**. (c) Structure of {Mo_{152}} in **8**. The oxygen atoms contributing to the intercluster connections and Mo atoms in the next cluster that bond to them are shown with larger spheres. Site occupancy of {Mo_2} marked with blue circle is 0.5.

mixture in accordance with eq 1. Although the pH dependence of nuclearity of smaller polyoxometalates have been successfully investigated by potentiometric, spectrometric, and/or electrochemical investigations,[35,37,38] these methods can hardly characterize higher nuclearity complexes like the ones studied here. Single crystal X-ray diffraction seems the only practical technique that can provide unambiguous speciation of these complexes. Successful crystallization of a series of {Mo_{154-x}} clusters has allowed us to examine the pH dependence of the nuclearity of the clusters that precipitate from the solutions at various pH.

In the crystals **1**−**8**, the difference in the nuclearity was solely associated with the defect of the {Mo_2} linkers, unlike the acetate containing rings where defects of the {Mo_1} moiety also account for the nuclearity change. The structure of {Mo_{138}} exemplifies that an arrangement of adjoining two {Mo_2} defects is possible, although it is the first place to be filled by an additional linker upon nuclearity growth to {Mo_{142}}. Some higher nuclearity clusters cannot be obtained by simple addition of {Mo_2} linkers to lower nuclearity ones, which implies that the nuclearity growth of these clusters involve not only the additions but also the dissociations of the {Mo_2} linkers. This nuclearity-growth mechanism involving stepwise and reversible additions and dissociations of {Mo_2} linkers may account for the formation of {Mo_{138}} with eight {Mo_2} defects, the existence of which was excluded by the mechanism via irreversible condensation of {Mo_{20}} and {Mo_{21}} units where the dissociation of {Mo_2} during the nuclearity growth was not taken into account.[30]

The presence and absence of the {Mo_2} linkers affect the structure of the anion in two ways: the deviation from the 7-fold symmetry and the thickness of the ring. The former can be estimated by examining the distances between the central Mo atoms of the {(Mo)Mo_5} pentagonal units (Mo1), as summarized in Table 3. In the crystals **1**−**5** where all the occupancies of the {Mo_2} linkers are either 1 or 0, Mo1−Mo1 distances are 13.06(7) Å for the pairs of {Mo_{11}} repeating units between which the {Mo_2} units are present and about 12.53(11) Å for those between which the {Mo_2} units are absent. This indicates that the {Mo_2} unit is slightly larger than the size of the defect. This effect gives rise to the second effect: the thickness of the ring depends on the number of the defects. The {Mo_2} linkers squeezed into the defect sites are shifted away from the best plane of the ring to reduce the steric repulsion and thus the ring becomes thicker. This effect can be seen in the deviation of the Mo atoms of linker units measured from the best plain of the ring. The linkers with their neighboring sites left vacant (all linkers in crystals **1**−**3** and Mo8A−Mo7B in crystals **4**−**5**) show smaller deviations, as shown in Figure 8.

Geometry of Extended Structures. All the crystals **1**−**5** and **7** and {$Mo_{138}(CH_3CO_2)_6$}[33] belong to the same space group type of *C*2/*m*. These structures are achieved by arranging the centers of giant cluster anions at the *C*-centered monoclinic lattice points and aligning their C_2 axes along the crystallographic *b* axes (thus aligning their axle in the *ac* plane). The site symmetry of each anion is 2/*m*. Crystal **6** belongs to a different space group *C*2/*c*, which however is a type IIb *klassengleiche* subgroup of *C*2/*m*. The structure of **6** could be interpreted as a slightly distorted structure where the axle of the ring is slightly tilted from the *ac* plane to reduce the crystallographic site symmetry of the anions from 2/*m* to $\bar{1}$. These packing patterns seem to be a common packing pattern of this kind of giant rings, and each structure can be characterized by the unit cell dimensions and the angle of the axle with respect to the crystallographic *a* axis (plus the degree of tilting in the case of crystal **6**).

In the crystals **2**, **3**, and **6**−**8**, the {Mo_{154-x}} anions are connected into one-, two-, or three-dimensional extended structures. Comparison of the extended structures of crystals **1**−**8** with the pH of their synthetic conditions does not show apparent correlation either with the number of intercluster bonds or with the geometry of the extended structures, as summarized in Table 2. Thus eq 2 does not seem to be a good guiding principle in controlling the geometry of extended structures, in contrast to eq 1 that successfully explained the pH dependence of the nuclearity of the clusters.

Distribution of Defect Sites and Intercluster Connection Modes. Inspection of these structures from a tectonic point of view reveals the relationship between the distribution of the

(37) Sasaki, Y.; Sillén, L. G. *Ark. Kemi* **1967**, *29*, 253–277.
(38) Pettersson, L.; Hedman, B.; Andersson, I.; Ingri, N. *Chem. Scr.* **1983**, *22*, 254–264.

Table 3. Distances between the Mo1 Atoms of Adjoining Repeating Units in Crystals **1**−**8**

ID of the repeating unit	{Mo_{138}} in **1**	{Mo_{138}} in **2**	{Mo_{138}} in **3**	{Mo_{142}} in **4**	{Mo_{142}} in **5**	{Mo_{148}} in **6**	{Mo_{150}} in **7**	{Mo_{150}} in **8**	{Mo_{152}} in **8**[e]
A−A′	13.115(1)	13.040(3)	13.015(2)	12.645(5)[a]	12.427(1)[a]	12.856(2)[b,c]	12.824(1)[c]	12.864(3)[b]	12.788(2)
A−B	12.512(1)[a]	12.284(2)[a]	12.566(1)[a]	13.186(3)	13.076(1)	12.734(2)[c]	12.917(1)	12.840(2)	12.780(2)
B−C	13.096(1)	13.094(2)	13.089(1)	12.510(3)[a]	12.563(1)[a]	12.896(2)	12.684(1)	12.853(2)	12.863(2)
C−D	12.696(1)[a]	12.585(2)[a]	12.520(1)[a]	12.972(3)	12.945(1)	12.786(2)	12.891(1)[d]	12.856(3)	12.889(2)
D−E						12.919(2)		12.864(3)[d]	12.850(2)
E−F						12.834(2)		12.783(3)[d]	12.530(2)[c]
F−G						12.775(2)[c]		12.730(3)[c]	12.945(2)

[a] The {Mo_2} linker between these units is missing. [b] Showing the distance between Mo1 of units G and A. [c] Site occupancy of the {Mo_2} linker between these units is 0.5. [d] Site occupancy of the {Mo_2} linker between these units is 0.75. [e] In this column, distances between Mo1 of units N−H, H−I, I−J, J−K, K−L, L−M, and M−N are listed.

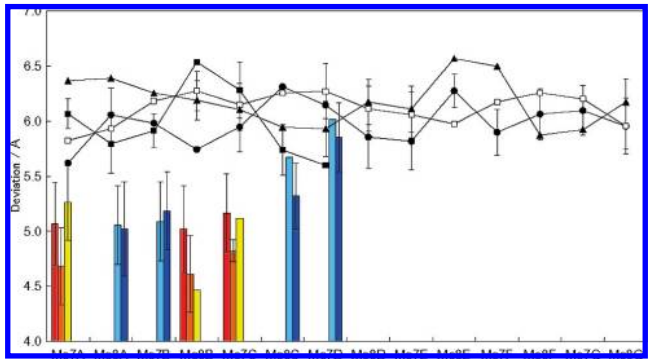

Figure 8. Deviation of the Mo atoms in {Mo_2} linkers from the least-squares plane defined by 14 Mo9 atoms. Red bar, {Mo_{138}} in crystal **1**; orange bar, {Mo_{138}} in crystal **2**; yellow bar, {Mo_{138}} in crystal **3**; light blue bar, {Mo_{142}} in crystal **4**; dark blue bar, {Mo_{142}} in crystal **5**; filled circle, {Mo_{148}} in crystal **6**; filled square, {Mo_{150}} in crystal **7**; open square, {Mo_{150}} in crystal **8**; filled triangle, {Mo_{152}} in crystal **7**. Where the Mo atom is disordered over two sites, average deviation is shown with an error bar each end of which indicates the individual deviation.

{Mo_2} defects in the constituent clusters and the intercluster connection modes. In the two-dimensional aggregation of {Mo_{138}} in crystals **2** and **3**, the intercluster connection involves four Mo atoms of each cluster, of which two belong to an {Mo_2} linker unit and two belong to the pentagonal units on its both sides, as shown in Figure 3. This connection mode was observed in {Mo_{146}}[19] and {Mo_{144}}.[26] It would cause steric repulsion at the neighboring {Mo_2} units and is therefore possible only when both of them are lacking to form a sequence of three {Mo_2} sites with the presence of a linker at the center and the defects at both ends. In crystals **1**−**8**, such sequences are present only in {Mo_{138}} and {Mo_{142}}. {Mo_{138}} has four of those that are separate from each other, thus the cluster can extend intercluster connections to four directions to form a two-dimensional aggregation. On the other hand, two sequences on each side of {Mo_{142}} share a defect site and thus only one of those is allowed to contribute to intercluster connection formation. Therefore, the two-dimensional aggregation using this connection mode is only possible for {Mo_{138}}.

In the three-dimensional framework in **6** and one-dimensional chain in **7**, the intercluster connection involves two Mo atoms from each cluster, which belong to two {Mo_2} units on both sides of a pentagonal unit, as shown in Figures 5 and 6. These connections tend to be located in the proximity of {Mo_2} defects. In crystal **6**, connections from units B and F involves linker sites X and Z that are absent at 50% probability. The connection from unit D has the linker site Y′ behind the ring that is absent at 50% probability. In crystal **7**, the connection from D is surrounded by linkers Y, Y′, and X′, one of which is absent on the average. However, the absence of proximal linker may not always be necessary for this type of intercluster connection since this mode was also observed in the linearly connected defect-free {Mo_{154}} chain.[22]

In the one-dimensional chain of {Mo_{152}} in **8**, the intercluster connection involves five O atoms from each cluster, of which three belong to a pentagonal unit and two belong to two {Mo_2} units on both sides of the pentagonal unit, as shown in Figure 7. There are no proximal defect {Mo_2} linkers around this connection. This connection mode was observed in {Mo_{146}}[19] and {Mo_{144}}.[26,39] The connection modes observed in crystals **6**−**8** require consecutive existence of two {Mo_2} sites and therefore prefer higher nuclearity clusters.

The relationship between the nuclearity of the constituent clusters and the network geometry indicates that the tectonic principle dominates the aggregation pattern. Although equation 2 does not directly govern the intercluster connection formation, the pH contributes to the three-dimensional network formation through controlling the nuclearity and the distribution of the {Mo_2} linkers and defects. It also indicates that additional components that either help defect formation or replace {Mo_2} linker units would lead to different aggregation patterns.

Concluding Remarks. In the simplest system of the {Mo_{154-x}} family ring-shaped polyoxomolybdate giant clusters, nuclearity of the cluster was demonstrated to be directly controlled by the solution pH of mother liquor. This principle will also apply to more complex systems containing additional components and will give a guide for designing new compounds. Geometry of the extended structure was not directly but was implicitly controlled by the pH. It is affected by the tectonics of the component clusters, the structures of which are governed by the solution pH. Exploitation of single crystal synchrotron X-ray diffraction has enabled this systematic set of structure analyses.

Experimental Section

Reagents. The following were purchased from commercial sources and used without further purification: 99% $(NH_4)_6Mo_7O_{24}\cdot 4H_2O$, 99% NH_4Cl, 35−37% hydrochloric acid (Wako), 98% hydrazinium dichloride (Kanto).

Sample Preparations. The crystals **1**−**8** were obtained from systematically prepared solutions: the pH of the 70 mL aqueous solution dissolving 2.00 g sample of $(NH_4)_6Mo_7O_{24}\cdot 4H_2O$ (1.62 mmol) was adjusted to 4.5, 4.2, 4.0, 3.5, 3.3 3.0, 2.5, 2.2, 1.7, and 1.4 with 1 or 2 mol dm^{-3} aqueous hydrochloric acid. To each solution, 42 mg sample of hydrazinium dichloride powder (0.40 mmol) was added, followed by stirring for 75 min. At pH 1.7 and 1.4, white crystals of $(NH_4)_8[Mo_{36}O_{112}(H_2O)_{16}]\cdot nH_2O$ ($n \approx 47$) precipitate at this stage but they were not removed from the solution. The solution was kept stationary at 15 °C. Dark blue plate crystals appeared after 2 to 7 weeks.

(39) Both {Mo_{144}}[26] and {Mo_{146}}[19] have two independent clusters, of which one is connected by four Mo-O-Mo bonds and the other by five Mo-O-Mo bonds.

Crystal Structure Determinations. All the crystals were subjected to synchrotron X-ray diffraction experiment using a Rigaku MERCURY CCD diffractometer at NW2A beamline of the Advanced Ring, Photon Factory (PF) of High Energy Accelerator Research Organization (KEK). Diffraction data were collected using CrystalClear[40] and processed by HKL2000.[41] Structures were solved by the direct method using SHELXS97 and refined by the full-matrix least-squares using SHELXL97.[42] Since it is extremely difficult to distinguish NH_4^+ cations from water molecules of crystallization in such large structures by the use of X-ray diffraction, all the atoms outside the clusters were refined by using the scattering factor of neutral oxygen atom. For the crystals **1**−**5** and **7**, all the Mo and O atoms of the {Mo_{154-x}} clusters were refined with anisotropic displacement parameters while the atoms outside the clusters were refined isotropically. For the crystals **6** and **8**, all the O and disordered Mo atoms were also set isotropic, since their anisotropic refinements were unstable because of the smaller contribution of each Mo atom to the total scattering intensity. The number of independent Mo atoms in crystals **6** and **8** are approximately double and quadruple compared with those in crystals **1**−**5** and **7**. The crystal data are summarized in Table 1. Chemical formulas of the clusters were estimated by the bond valence sum (BVS) calculations and assuming the oxidation states of Mo to be +5 for 28 atoms and +6 for the rest.[20] Bond valence values were calculated using the equation and parameters given by Brown and Altermatt.[43] When calculating the BVS of an O atom coordinating to a Mo atom that is disordered over two sites, only the bond to the major site was taken into account and the contribution of the minor site was neglected. Oxygen atoms with BVS less than 0.50 were assigned to H_2O, those with BVS between 0.50 and 1.30 were assigned to OH^- and the other O atoms were assigned to O^{2-}. All the crystals **1**−**8** show packing coefficients[44,45] in the range of 41.55−55.8% (Table S3), indicating that a large amount of water molecules remains undetermined under the current analyses. Most of them are presumably severely disordered, even under temperature as low as 35 K.

Acknowledgment. Dedicated to Professor Tadashi Matsushita on the occasion of his retirement. This work was supported by CREST, Japan Science and Technology Agency and Grant-in-Aid for Scientific Research (Exploratory Research No. 18655022 and Priority Areas No. 19027019, Synergy of Elements) from the Ministry of Education, Culture, Sports, Science and Technology (MEXT). The synchrotron radiation experiments were performed under the approval of the Photon Factory Program Advisory Committee (Proposal Nos. 2003G186 and 2005G153). Authors thank Professor Shin-ichi Adachi for his help during the synchrotron radiation experiment.

Supporting Information Available: X-ray crystallographic files in CIF format for the crystals **1**−**8**. Table S1 lists a survey of hitherto reported structurally characterized {Mo_{154}} derivatives with their key synthetic parameters and the resultant structural features. Table S2 lists deviations of the Mo atoms of {Mo_2} linker units (Mo7 and Mo8) from the best planes determined by 14 Mo9 atoms. Table S3 lists packing coefficients of crystals **1**−**8**. Figures S1−S8 show the packing diagrams of crystals **1**−**8**. This material is available free of charge via the Internet at http://pubs.acs.org.

JA800784A

(40) *CrystalClear*; Molecular Structure Corporation: Orem, UT, 2001.
(41) Otwinowski, Z.; Minor, W. *Methods Enzymol.* **1997**, *276A*, 307–326.
(42) Sheldrick, G. M. *Acta Crystallogr., Sect. A* **2008**, *64*, 112–122.
(43) Brown, I. D.; Altermatt, D. *Acta Crystallogr., Sect. B* **1985**, *41*, 244–247.
(44) Spek, A. L. *PLATON, A Multipurpose Crystallographic Tool*; Utrecht University: Utrecht, The Netherlands, 1985.
(45) Kitaigorodski, A. I. *Organic Chemical Crystallography*; Consultants Bureau: New York, 1961.